INTERNATIONAL JOURNAL OF CLIMATOLOGY
Int. J. Climatol. **35**: 4276–4292 (2015)
Published online 16 February 2015 in Wiley Online Library
(wileyonlinelibrary.com) DOI: 10.1002/joc.4285

RMetS
Royal Meteorological Society

Projections of climate change in the Mediterranean Basin by using downscaled global climate model outputs

Tugba Ozturk,[a,b] Zeynep Pelin Ceber,[c] Murat Türkeş[d]* and M. Levent Kurnaz[a]

[a] *Department of Physics, Faculty of Science and Arts, Bogazici University, Istanbul, Turkey*
[b] *Department of Physics, Faculty of Science and Arts, Isik University, Istanbul, Turkey*
[c] *Institute of Environmental Sciences, Bogazici University, Istanbul, Turkey*
[d] *Affiliated Faculty at the Department of Statistics, Middle East Technical University, Ankara, Turkey*

ABSTRACT: The Mediterranean Basin is one of the regions that shall be affected most by the impacts of the future climate changes on hydrology and water resources. In this study, projected future changes in mean air temperature and precipitation climatology and inter-annual variability over the Mediterranean region were studied. For performing this aim, the future changes in annual and seasonal averages for the future period of 2070–2100 with respect to the period from 1970 to 2000 were investigated. Global climate model outputs of the World Climate Research Program's Coupled Model Intercomparison Project Phase 3 multi-model dataset were used in this work. Intergovernmental Panel on Climate Change SRES A2, A1B and B1 emission scenarios' outputs were used in future climate model projections. Future surface mean air temperatures of the larger Mediterranean basin increase mostly in summer and least in winter, and precipitation amounts decrease in all seasons at almost all parts of the basin. Future climate signals for air temperature and total precipitation values are much larger than the inter-model standard deviation. Inter-annual temperature variability increases evidently in summer season and decreases in the northern part of the domain in the winter season, while precipitation variability increases in almost all parts of domain. Probability distribution functions are found to be shifted and flattened for future period compared to the reference period. This indicates that the occurrence of frequency and intensity of high temperatures and heavy precipitation events will likely increase in the future period.

KEY WORDS Mediterranean Basin; Turkey; climate change and variability; air temperature; precipitation; emission scenarios; climate model simulation

Received 17 April 2014; Revised 12 January 2015; Accepted 15 January 2015

1. Introduction

Climate change is one of the most significant and far-reaching challenges that human societies have faced in this century. The evidence of human-induced climate change has been getting stronger on different spatial and temporal scales. Climate change has been damaging the ecological, social and economic systems. According to the fifth scientific assessment report of the Intergovernmental Panel on Climate Change (IPCC) (Stocker *et al.*, 2013), each of the last three decades has been successively warmer at the Earth's surface than any preceding decade since 1850. In the Northern Hemisphere, 1983–2012 was likely the warmest 30-year period of the last 1400 years. According to the report, the globally averaged combined land and ocean surface temperature data as calculated by a linear trend, show a warming of 0.85 [0.65–1.06] °C, over the period 1880–2012, according to multiple independently produced datasets. The total increase in temperature between the average of the 1850–1900 period and the 2003–2012 period is 0.78 [0.72 to 0.85] °C, based on the single longest dataset available. According to the report, time series of projected temperature change relative to 1986–2005 averaged over land grid points in the South Europe and the Mediterranean (30°N to 45°N, 10°W to 40°E) regions shows that it is likely that there will be an increase between 2 and 3 °C under the RCP4.5 scenario and between 4 and 6 °C under the RCP8.5 scenario. It also says that decreased precipitation in the Mediterranean, Caribbean and Central America, southwestern United States and South Africa is likely under the RCP8.5 scenario, and is projected with medium confidence to be larger than natural variations by the end of the 22nd century in some seasons.

Other climate variables are also changing such as precipitation amounts and variability, snow and ice cover patterns and mean sea level. Precipitation is highly variable spatially and temporally, and precipitation data are limited in some regions. Significantly decreased precipitation amounts (drying) were observed particularly in the Sahel and the Mediterranean Basin including Turkey (Tomozeiu *et al.*, 1995; Esteban-Parra *et al.*, 1998; Türkeş, 1998, 1999; Buffoni *et al.*, 1999, 2000; Gonzalez-Rouco *et al.*, 2000, 2001; Xoplaki *et al.*, 2000; Houghton *et al.*, 2001; Giorgi, 2002; Türkeş and Erlat, 2005; Trigo *et al.*, 2006; Solomon *et al.*, 2007; Tatlı and Türkeş, 2008, 2011a,

* Correspondence to: M. Türkes, Affiliated Faculty at the Department of Statistics, Middle East Technical University (METU), Ankara 06800, Turkey. E-mail: murat.turkes57@gmail.com

2011b; Türkeş and Tatlı, 2009, 2011; Türkeş *et al.*, 2009; etc.). Substantial increases in heavy precipitation events have also been observed.

Dry summer subtropical Mediterranean climates can be found along the west coasts of the continents between about 25° and 40° latitude (Türkeş, 2010). The Mediterranean macro climate mainly results from the seasonal alternation between mid-latitude (frontal) cyclones, associated with polar air masses, during the winter and subtropical high pressure systems, from subsiding maritime and continental tropical air masses during the summer. The major characteristic of the Mediterranean climate is of high temporal variability varying from seasonal and inter-annual to centennial scales because it extends in a transition region between temperate and cold mid-latitudes and Tropics (i.e. subtropical zone); it has been facing significant circulation (associated pressure and wind systems characterizing mid-latitude and tropical/monsoonal weather and climate, respectively) changes between winter and summer. It is closely associated with several atmospheric oscillation and/or teleconnection patterns during the year also varying depending on seasons, such as North Atlantic Oscillation (NAO), Arctic Oscillation (AO), Med. Oscillation (MO), El Niño-Southern Oscillation (ENSO), and North Sea–Caspian Pattern (NCP), and so on (Kutiel *et al.*, 2002; Hurrell *et al.*, 2003; Türkeş and Erlat, 2003, 2006, 2008, 2009; Kutiel and Türkeş, 2005; Trigo *et al.*, 2006; etc.). Mediterranean climate receives major influence from sea and land distribution and the interactions between sea and lands, in addition to the ocean–atmosphere interaction, during the year particularly in the 'true' or 'actual' Mediterranean macro climate region. Therefore, the larger Mediterranean Basin is very important and among the most responsive regions to global climate change. There were many studies consisting of ensembles of global (Kittel *et al.*, 1998, Giorgi and Francisco, 2000; Giorgi *et al.*, 2001; Giorgi and Bi, 2005a, 2005b; Giorgi, 2006, Kripalani *et al.*, 2007; Giorgi and Lionello, 2008; Sheffield and Wood, 2008; Lelieveld *et al.*, 2012; etc.) and regional (Machenhauer *et al.*, 1998; Deque *et al.*, 2005; etc.) climate model simulations including the Mediterranean Basin. Regional climate change projections over the Europe, including totally or partially the Mediterranean Basin were presented by several studies (e.g. Giorgi *et al.*, 1992; Giorgi *et al.*, 1997; Jones *et al.*, 1997; Rotach *et al.*, 1997; Deque *et al.*, 1998; Raisanen *et al.*, 1999; Christensen and Christensen, 2003; Giorgi *et al.*, 2004; Kjellstrom, 2004; Pal *et al.*, 2004; Raisanen *et al.*, 2004; Schar *et al.*, 2004; Semmler and Jacob, 2004; Deque *et al.*, 2005; Gao *et al.*, 2006; Beniston *et al.*, 2007; Kjellstrom *et al.*, 2007; Alpert *et al.*, 2008; Gao and Giorgi, 2008; Ozturk *et al.*, 2012, 2013; etc.) where the area is considered as a climate change hotspot.

There have been many experiments consisting of global and regional climate projections for all parts of the world (Table 1). There are also some studies performing simulation by using one regional climate model (Semmler and Jacob, 2004; Gao *et al.*, 2006; Alpert *et al.*, 2008; etc.). Multi-model ensemble simulations results showed that the Mediterranean Basin will be seriously affected by severe climate conditions (Table 1).

In this study, we have detected the projected future changes and variability in annual and seasonal averages of the surface mean air temperatures and total precipitation amounts for the Mediterranean macroclimate region, by using 16 global models with three emission scenarios. The study region covers the Mediterranean Basin as a whole from the North Atlantic to Syria and from the North Africa to the South Europe including Turkey and the Black Sea Basin. Projected future changes include the period of 2070–2100 in comparison with present climate (1970–2000), which have been estimated by 16 global climate model (GCM) outputs from the World Climate Research Program's (WCRP's) Coupled Model Intercomparison Project Phase 3 (CMIP3) multi-model dataset (Meehl *et al.*, 2007) with three different emission scenarios of the IPCC (Nakicenovic and Swart, 2000), including A2, A1B and B1. Sixteen GCMs were downscaled to 50 km resolution by using the bias-correction and spatial downscaling method (Wood *et al.*, 2004). Although there are many studies of GCM ensembles (Christensen and Christensen, 2003; Giorgi, 2006; Giorgi and Bi, 2005a, 2005b; Giorgi and Lionello, 2008), they are not in such a high resolution of 50 km because the resolution of global model simulations varies in the range of 100–500 km. There is a mismatch between the grid resolution of current GCMs whose resolution is generally a few hundred kilometers, and the resolution necessary for environmental impacts models (typically 10 km or less). To assess the impacts of climate change on ecological processes, climate scenarios with sufficient spatial resolution represent the varying effects of climate change on physical, biological and cultural landscapes (Tabor and Williams, 2010). One of the important outcomes of the study by Gao *et al.* (2006) is that the climate change signal over the Mediterranean region shows significant fine-scale structure due to the complex topography of the region. Therefore, downscaling is needed, as the processes described by the environmental impact models are very sensitive to the local climate variations, such as topography, which is not captured at coarse scales (Maurer and Hidalgo, 2007).

Ensemble means of global model data provide us robustness of results and allow a much better assessment of climate change projections. They enable us to address the issues regarding uncertainty due to model configuration. In order to assess the trends across models, we presented the ensemble mean and inter-model standard deviation of the 21st century trends in mean and variability changes. We investigated the result of a wide range of GCMs to produce climate change projections over the Mediterranean region.

2. Data and methodology

2.1. Datasets

We used 16 GCM outputs, which are shown in Table 2, for temperature and precipitation from the WCRP's

Table 1. Summary of the experiments including global and regional climate projections for all parts of the world.

Region	Source	Time periods	Emissions scenarios	Overall findings	Reference
Global	20 GCMs	2080–2099	SRES A1B, A2 and B1	Mediterranean and North Eastern European regions are the two most prominent Hot-Spots emerging from the Regional Climate Change Index (RCCI) analysis. The greatest contribution to the Mediterranean RCCI is given by a large decrease in mean precipitation and an increase in precipitation variability during the dry (warm) season. This summer drying signal that makes the Mediterranean one of the most responsive regions to global change has been consistently observed in different generations of model projections	Giorgi, 2006
Eastern Mediterranean and the Middle East	HadRM3P	2070–2099	SRES A1B	• Daytime maximum temperatures appeared to increase most rapidly in the Balkan Peninsula and Turkey • Hot summer conditions that rarely occurred in the reference period may become normal by the middle and end of the 21st century • Annual precipitation totals were expected to decrease in the southern Europe and Turkey regions and the Levant, whereas in the Arabian Gulf area it may increase	Lelieveld *et al.*, 2012
Mediterranean	HadAM3H	2071–2100	SRES A2 and B2	Particularly the central and southern portions of the Iberian peninsula, and Italian, Hellenic and Anatolia peninsulas and areas of south-eastern Europe (e.g. Romania and Bulgaria), the Middle East, northern Africa and major Islands (Corsica, Sardinia and Sicily) will be affected due to a large warming and pronounced decrease in precipitation, especially during the spring and summer seasons	Gao and Giorgi, 2008
Europe	PRUDENCE Model Data	2071–2100	SRES A2 and B2	• Countries in Central Europe will experience the same number of hot days as they are currently experiencing in southern Europe • Intensity of extreme temperatures increases more rapidly than the intensity of more moderate temperatures over the continental interior • Heavy winter precipitation increases in Central and Northern Europe and decreases in the south and heavy summer precipitation increases in north-eastern Europe and decreases in the south	Beniston *et al.*, 2007
Europe	HIRHAM4	2071–2100	SRES A2	Increase in the amount of precipitation that exceeds the 95th percentile in many areas of Europe, despite a possible reduction in average summer precipitation over a substantial part of the continent	Christensen and Christensen, 2003
Mediterranean	17 AOGCMs	2071–2100	SRES A1B, A2 and B1	Projected decrease in precipitation amounts, especially in the summer season, except for some northern Mediterranean regions (e.g. the Alps) in winter, a pronounced warming, which is the biggest in the summer season, and increase in inter-annual variability especially in summer	Giorgi and Lionello, 2008

Table 2. A list of the global climate models used in the study.

GCM DATA	Centre	Country
BCCR-BCM2.0	Bjerknes Centre for Climate Research	Norway
CGCM3.1 (T47)	Canadian Center for Climate Modelling and Analysis	Canada
CNRM-CM3	Centre National de Recherches Meteorologiques	France
CSIRO-Mk3.0	Australia's Commonwealth Scientific and Industrial Research Organization	Australia
GFDL-CM2.0	Geophysical Fluid Dynamics Laboratory	USA
GFDL-CM2.1	Geophysical Fluid Dynamics Laboratory	USA
GISS-ER	Goddard Institute for Space Studies	USA
INM-CM3.0	Institute for Numerical Mathematics	Russia
IPSL-CM4	Institut Pierre Simon Laplace	France
MIROC3.2 (medres)	National Institute for Environmental Studies	Japan
ECHO-G	Meteorological Institute, University of Bonn	Germany
ECHAM5/MPI-OM	Max-Planck-Institute for Meteorology	Germany
MRI-CGCM2.3.2	Meteorological Research Institute	Japan
PCM	National Centre for Atmospheric Research	USA
CCSM3	National Centre for Atmospheric Research	USA
UKMO-HadCM3	UK Met. Office	UK

Coupled Model Intercomparison Project Phase 3 (CMIP3) multi-model dataset (Meehl *et al.*, 2007). Climate model outputs were obtained from http://www.engr.scu.edu/~emaurer/global_data/ with IPCC emission scenarios of A2, A1B and B1 (Nakicenovic and Swart, 2000) for temperature and precipitation. These data were also downscaled as described by Maurer *et al.* (2009), by using the bias-correction and spatial downscaling method (Wood *et al.*, 2004). They have a 0.5 degree grid resolution based on the 1950–1999 gridded observations of Adam and Lettenmaier (2003). Time period of monthly downscaled data is 1950–2099. There are IPCC emission scenario A2 (850 ppm CO_2 concentration by 2100), A1B (700 ppm CO_2 concentration by 2100) and B1 (550 ppm CO_2 concentration by 2100) outputs of each global model for future analysis (Nakicenovic and Swart, 2000). By using global model outputs, we studied future changes (2070–2100) and variability of climate variables of annual seasonal mean surface air temperature and total precipitation for the Mediterranean macro region with respect to the present period (1970–2000). Ensemble averages of global model outputs were calculated by first performing the calculations for the individual models and then compute the ensemble average (Coppola and Giorgi, 2010).

2.2. Modelling and downscaling

Due to coarse spatial scale of GCM outputs, it is necessary to use some type of downscaling to characterize climate over small areas. In this study, bias-corrected and statistically downscaled monthly precipitation and temperature output from each GCM was used. GCM outputs were downscaled to a 1/2° grid by using an empirical statistical technique. The method maps the probability density functions for the monthly mean GCM precipitation and temperature onto those of gridded observed data for 1950–1999, aggregated to the 2° GCM scale. For bias removal, a quantile-based mapping (Panofsky and Brier, 1968) was constructed from the GCM climatology to the observed monthly climatology for average temperature and total precipitation. This same mapping is applied to the future GCM simulations as well. It allows the mean and variability of each GCM to evolve in agreement with the simulation, and all statistical moments between the GCM and observations for 1950–1999 also matches (Maurer *et al.*, 2009). This technique has compared favourably to different statistical and dynamic downscaling techniques (Wood *et al.*, 2004). According to the most significant findings of Wood *et al.* (2004), bias-correction and spatial disaggregation methods were successful in reproducing the main features of the observed hydrometeorology from the past climate simulation. Climate model outputs were not useful for hydrologic simulation purposes without a bias-correction step. For the future climate scenario, only the bias-correction and spatial disaggregation methods were able to produce hydrologically plausible results (Wood *et al.*, 2004). However, studies further suggest that to bias correct climate model output is needed to assure meaningful results in applications like hydrologic and water resources assessments (Kidson and Thompson, 1998; Murphy, 1999; Wilby *et al.*, 2000). The bias-correction and spatial disaggregation methods have been used successfully for projections in hydrologic impact studies (Wood *et al.*, 2002; Van Rheenan *et al.*, 2004; Maurer and Duffy, 2005; Hayhoe *et al.*, 2007; Sharma *et al.*, 2007; Barnett *et al.*, 2008; Vidal and Wade, 2008).

3. Results

3.1. Projected changes in mean and inter-annual variability

We presented ensemble averages of temperature change projections for the future period 2070–2100 with respect to the present period 1970–2000 based on the IPCC's A2, A1B and B1 emission scenarios in Figures 1–3, respectively. We investigated model ensemble future changes for four climatological seasons,

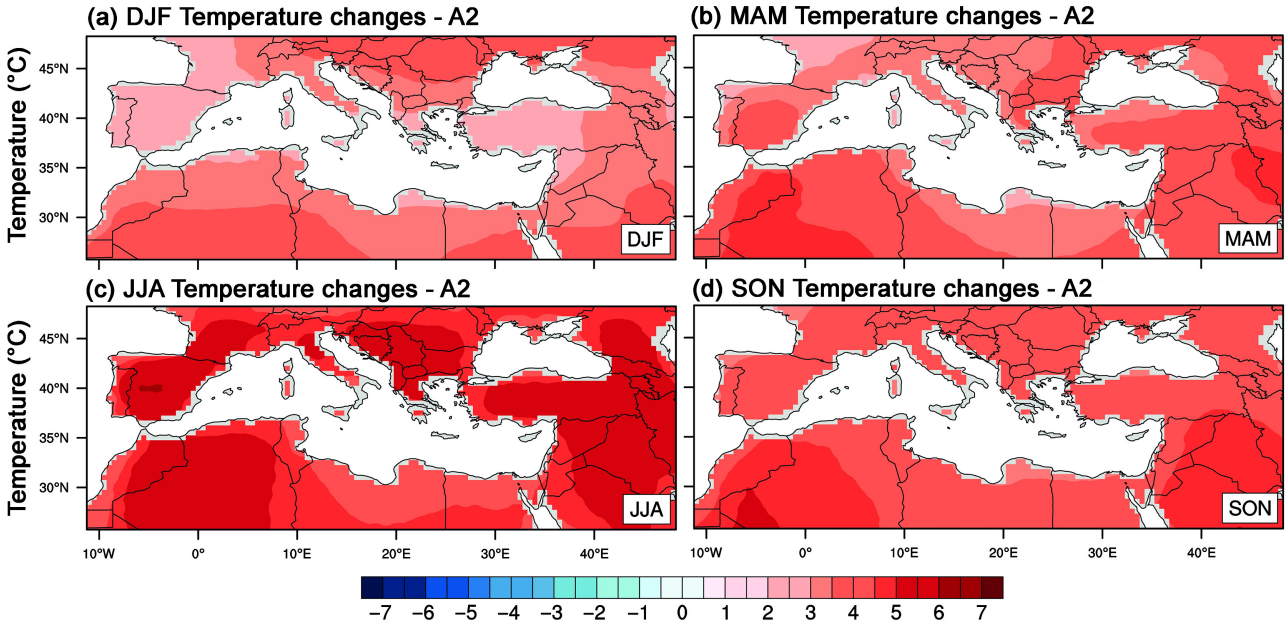

Figure 1. Ensemble average surface air temperature changes during the future period of 2070–2100 compared to present period of 1970–2000 based on the A2 scenario for CMIP3 GCMs in (a) winter (DJF: December–January–February), (b) spring (MAM: March–April–May), (c) summer (JJA: June–July–August), and (d) autumn (SON: September–October–November).

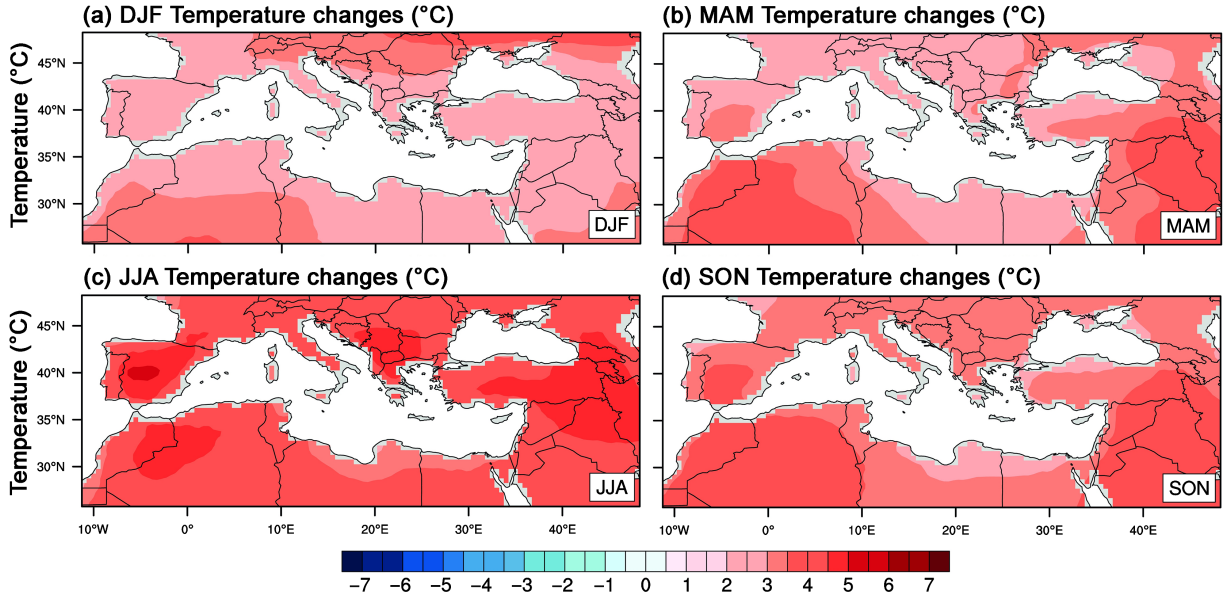

Figure 2. Ensemble average surface air temperature changes during the future period of 2070–2100 compared to present period of 1970–2000 based on the A1B scenario for CMIP3 GCMs in (a) winter (DJF: December–January–February), (b) spring (MAM: March–April–May), (c) summer (JJA: June–July–August), and (d) autumn (SON: September–October–November).

which are December–January–February (DJF, winter), March–April–May (MAM, spring), June–July–August (JJA, summer) and September–October–November (SON, autumn). According to all scenarios, surface air temperatures will very likely increase from a minimum of 1.5 to a maximum of 6.5 °C for all part of the Mediterranean region. According to a high-emission (or higher warming) scenario A2 of the IPCC, maximum warming of 6.5 °C is found in Turkey, Morocco, Algeria, southeast Europe and Iberian Peninsula in the summer season (Figure 1(c)). We observe more warming in North Africa and Central Europe in the winter season. For spring and autumn seasons, average surface air temperatures will very likely increase between 3.5 and 5.5 °C (Figure 1(b) and (d)). Warming or increased temperature pattern is coherent for all scenarios with maximum warming in summer and less warming in winter. According to a low emission (or lower warming) scenario B1 of the IPCC, warming range will be between a minimum 1.5 °C and a maximum 4 °C (Figure 3). Maximum temperature increase is again seen in summer same as in other scenario results mainly over the regions including south Balkans,

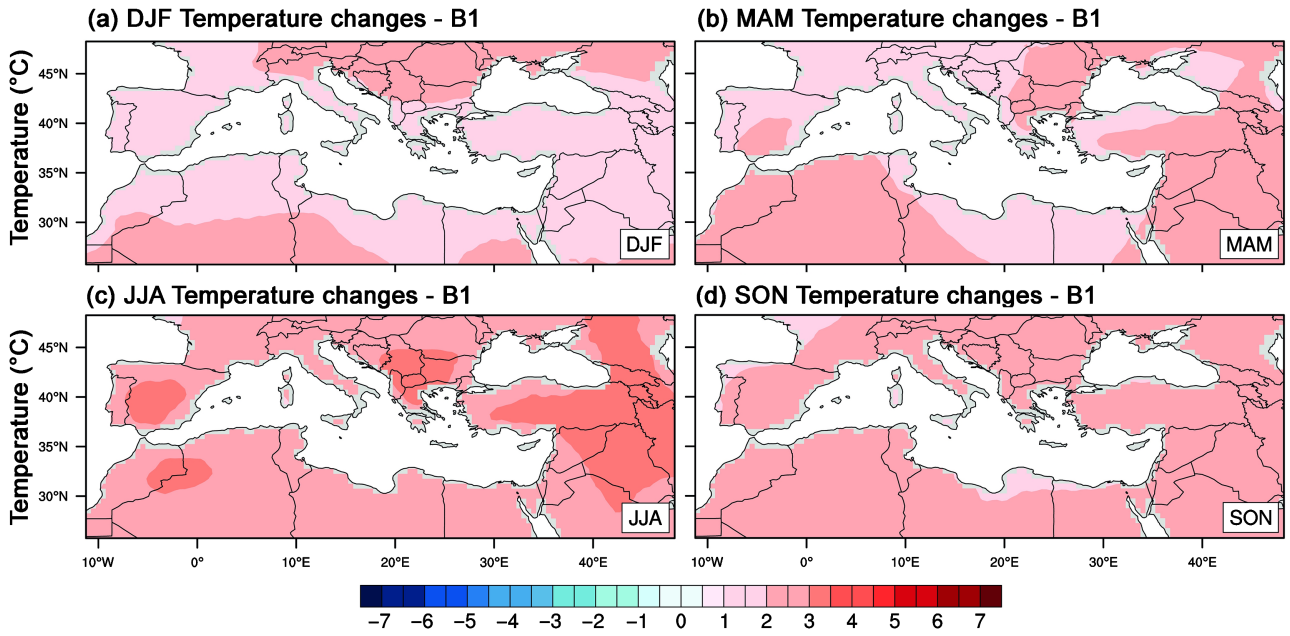

Figure 3. Ensemble average surface air temperature changes during the future period of 2070–2100 compared to present period of 1970–2000 based on the B1 scenario for CMIP3 GCMs in (a) winter (DJF: December–January–February), (b) spring (MAM: March–April–May), (c) summer (JJA: June–July–August), and (d) autumn (SON: September–October–November).

continental central, eastern and south-eastern Turkey, Caucasia and most of Middle East (Figure 3(c)).

Figures 4–6 show ensemble average precipitation change projections for the 2070–2100 period with respect to 1970–2000 normal according to the worst, A2, middle, A1B and best, B1 case scenarios, respectively. There will be a decrease in total precipitation series according to all three scenarios. Precipitation will decrease mostly in the northern part of the Mediterranean region including south Balkans, France, Italy and Caucasia in the summer season. An increase of 0.9 mm day^{-1} in precipitation is observed in Switzerland for the winter season. There will be a decrease from a maximum of 1.2 mm day^{-1} to a minimum of 0 mm day^{-1}. We observe a decreasing trend in continental central region for spring and autumn seasons as well.

Figure 7 shows the ensemble average temperature and precipitation change over the Mediterranean Basin for the future period of 2070–2100 with respect to the period of 1970–2000. Three different scenario (A2, A1B and B1) outputs of models are averaged over the domain for four seasons. The figure also includes the corresponding inter-model standard deviations of the changes. It gives the uncertainty in results due to use of different models. Results are consistent among A2, A1B and B1 scenario outputs. Change signal is highest in A2 scenario outputs, and lowest in B1 scenario output for temperature and precipitation. Uncertainty for temperature is much lower than the change itself, indicating that all changes are robust. Percentage of uncertainty with respect to the value of precipitation is greater than temperature; however it is still lower than the change itself.

Future changes in the year-to-year variability (i.e. inter-annual variation) of seasonal total precipitation amounts over Turkey were examined by the coefficient of variation (CV), which was calculated by taking the long-term standard deviation as a percentage of the long-term average of the precipitation series (Türkeş, 1998). However, the year-to-year variability of seasonal average mean air temperatures is expressed by the standard deviation of seasonal values (Türkeş and Erlat, 2008). Figures 8–10 show existence of ensemble average changes in inter-annual temperature variability for the period 2070–2100 with respect to the 1970–2000 normal. Changes are calculated for A2, A1B and B1 scenarios. We observe a decrease in variability in the northern part of the domain in winter for all three scenarios. However, temperature variability will increase in summer for all parts of the Mediterranean region according to A2 scenario outputs. For spring and autumn seasons, variability will increase in almost all parts of the domain as well, except for the Black Sea region.

Ensemble average changes in precipitation inter-annual variability for the period 2070–2100 with respect to the 1970–2000 normal for A2, A1B and B1 scenarios are shown in Figures 11–13. We observe a decrease in the variability in the south-eastern part of the domain during the summer season. However, a strong increase in precipitation variability is projected for A2 scenario output especially in the south part of the region (Figure 11). We have seen similar changes in other scenario (A1B and B1) outputs as well (Figures 12 and 13).

The statistical significance of equality of variances and means (long-term averages) of seasonal values of air temperatures and precipitation totals for reference and future periods was checked by the Levene test and Student's *t*-test. By using Levene test, the hypothesis that the two population variances are equal was rejected. The null

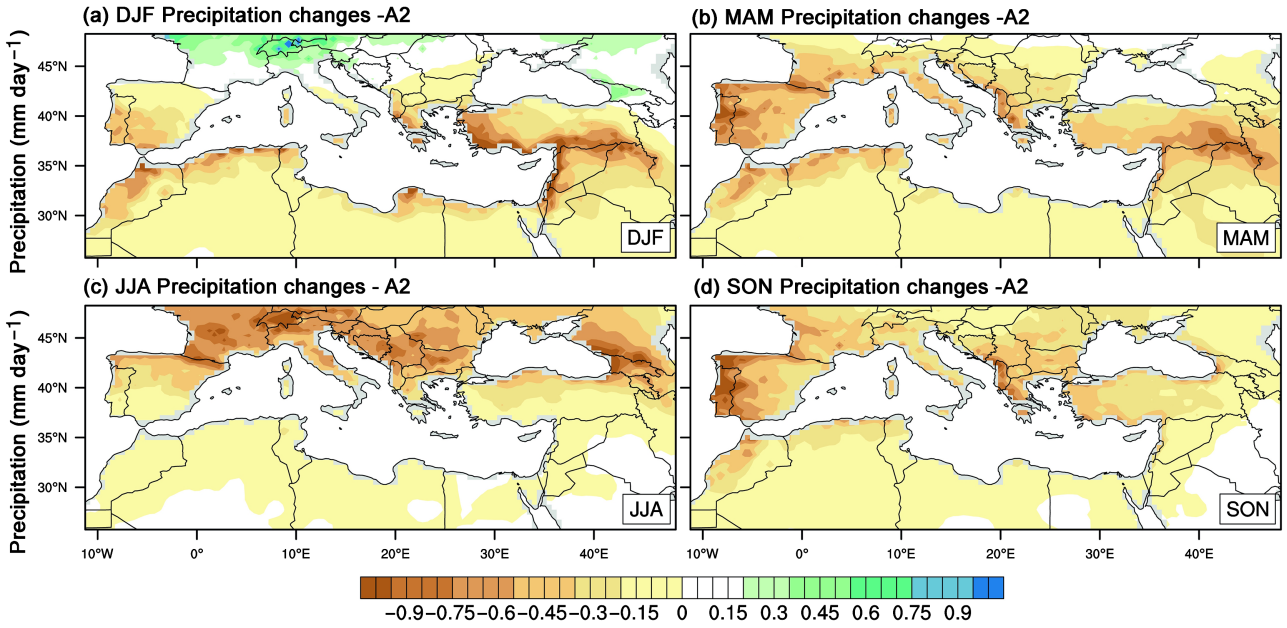

Figure 4. Ensemble average precipitation changes during the future period of 2070–2100 compared to present period of 1970–2000 based on the A2 scenario for CMIP3 GCMs in (a) winter (DJF: December–January–February), (b) spring (MAM: March–April–May), (c) summer (JJA: June–July–August), and (d) autumn (SON: September–October–November).

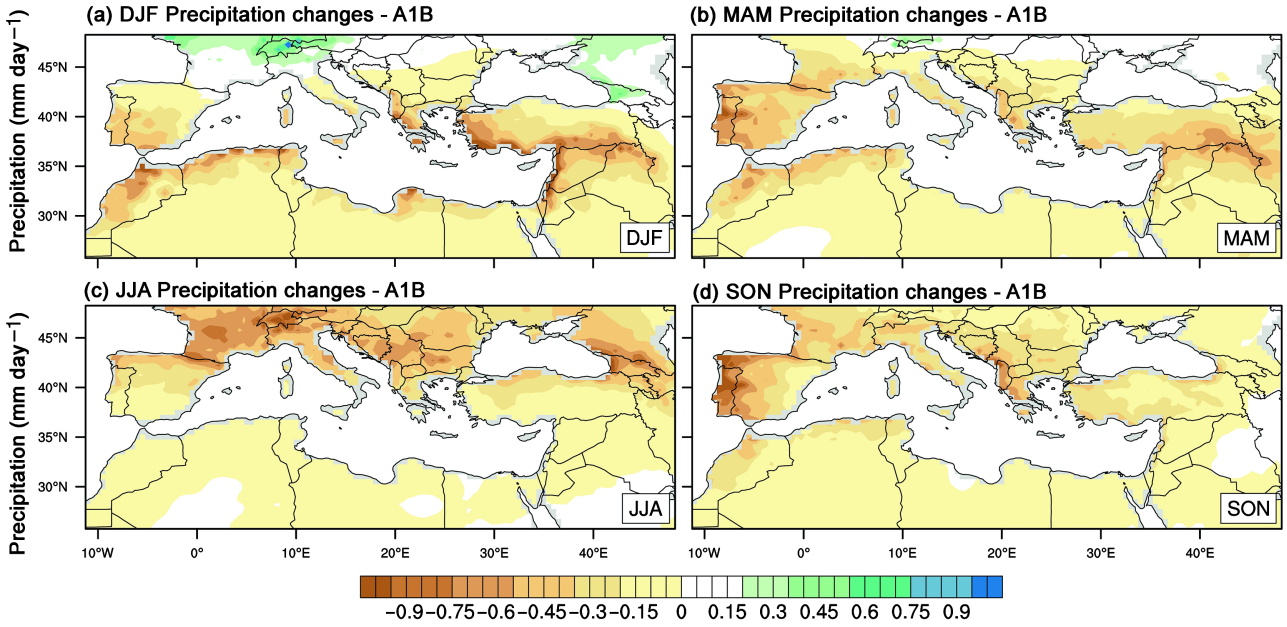

Figure 5. Ensemble average precipitation changes during the future period of 2070–2100 compared to present period of 1970–2000 based on the A1B scenario for CMIP3 GCMs in (a) winter (DJF: December–January–February), (b) spring (MAM: March–April–May), (c) summer (JJA: June–July–August), and (d) autumn (SON: September–October–November).

hypothesis of 'equal means assumed' was also rejected by using the Student's *t*-test. Even though significance level of the tests was chosen as 0.05, we have assessed the 0.01 and 0.001 levels of significance as well. According to the applied statistical test results, variances and mean values of seasonal averaged output of air temperature values and precipitation totals for future and reference period are quite different from each other. We have got similar results for all three scenario outputs (Table 3-only results for A2 scenario output was given here). Results evidently revealed that long-term averages and variances of seasonal air temperature and precipitation series will also very likely change statistically significant in future climate with respect to the climate of the reference period (Table 3).

3.2. Changes in the distribution of seasonal climate anomalies

We present the probability distribution functions (PDFs) of seasonal temperature and precipitation anomalies for the future and past periods in Figures 14 and 15. We have

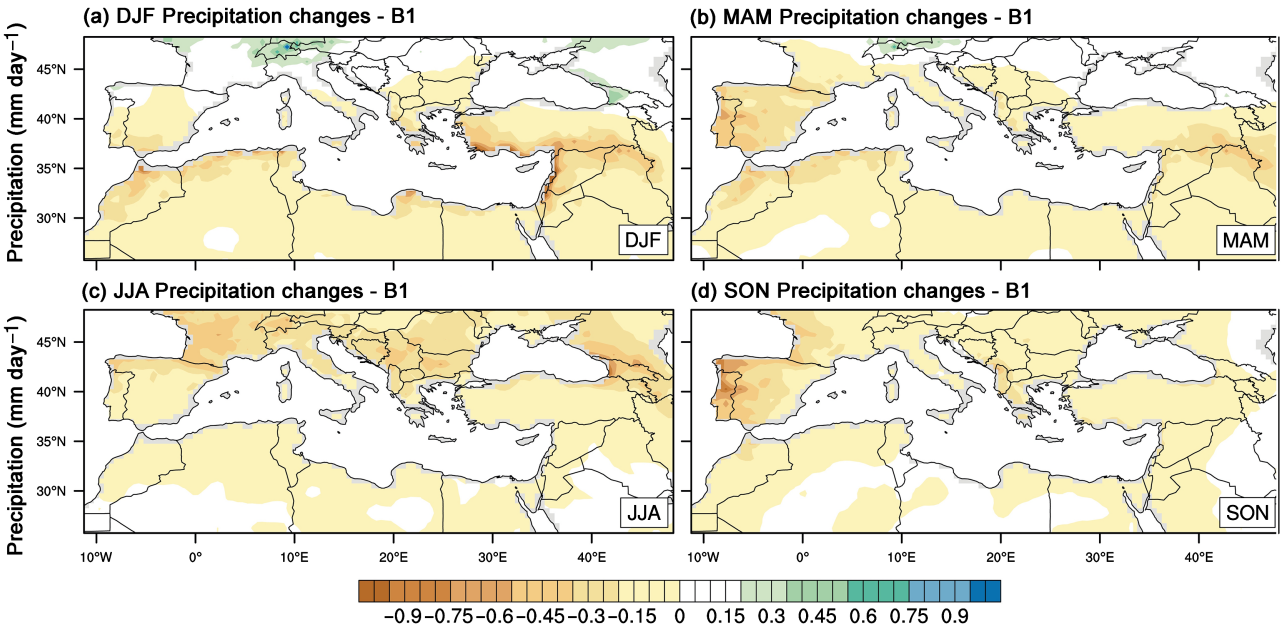

Figure 6. Ensemble average precipitation changes during the future period of 2070–2100 compared to present period of 1970–2000 based on the B1 scenario for CMIP3 GCMs in (a) winter (DJF: December–January–February), (b) spring (MAM: March–April–May), (c) summer (JJA: June–July–August), and (d) autumn (SON: September–October–November).

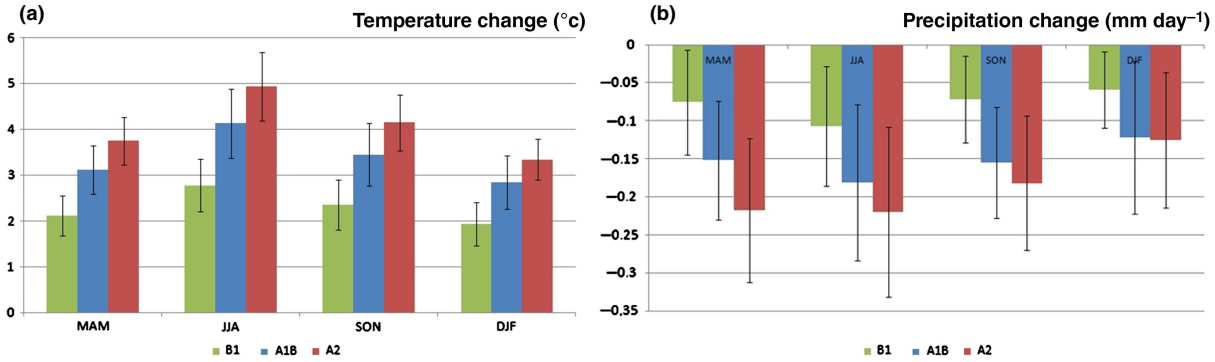

Figure 7. Ensemble average (a) surface air temperature (°C) and (b) total precipitation (mm day^{-1}) changes for the CMIP3 GCMs over the Mediterranean Basin based on the A2, A1B and B1 scenarios (2070–2100 to 1970–2000) with the corresponding inter-model standard deviations in winter (DJF), spring (MAM), summer (JJA) and autumn (SON).

prepared and displaced the histograms of yearly individual seasonal anomalies with respect to the ensemble average of the scenarios means for the reference period 1970–2000 for four seasons. Histograms of seasonal anomalies for future period of 2070–2100 with respect to reference period are also shown in the same graphs for all three scenario outputs. We represent seasonal anomalies in the unit of standard deviation (σ). Red, blue and green dashed lines represent A2, A1B and B1 seasonal anomalies, respectively. We tested normality distribution of the seasonal temperature and precipitation anomalies by using the Chi-square normality test. Results have shown that seasonal temperature anomalies for reference and future scenario outputs are normally distributed except in summer for A2 scenario output. Precipitation anomalies for reference and future periods for all scenario outputs are also normally distributed except in summer for A1B scenario output.

The descriptive statistics of the seasonal temperature and precipitation data are shown in Tables 4 and 5, respectively. We observe that skewness and kurtosis values of all data are close to zero indicating that they are normally distributed. Seasonal temperature and precipitation data distributions are approximately symmetric. The change in skewness is mostly positive in scenario outputs and data are skewed right indicating increase in frequency of warmer than average temperatures and higher than average precipitation. The kurtosis values of seasonal distributions decrease in most cases in future periods with respect to reference period indicating that distribution becomes flatter with increase in occurrence of warmer temperature and higher precipitation. Projected seasonal temperature and precipitation data indicate persistence at all seasons. This is indicated by the positive Lag 1 autocorrelation coefficients. Persistence of seasonal temperature data is statistically significant at the 0.001 level of significance.

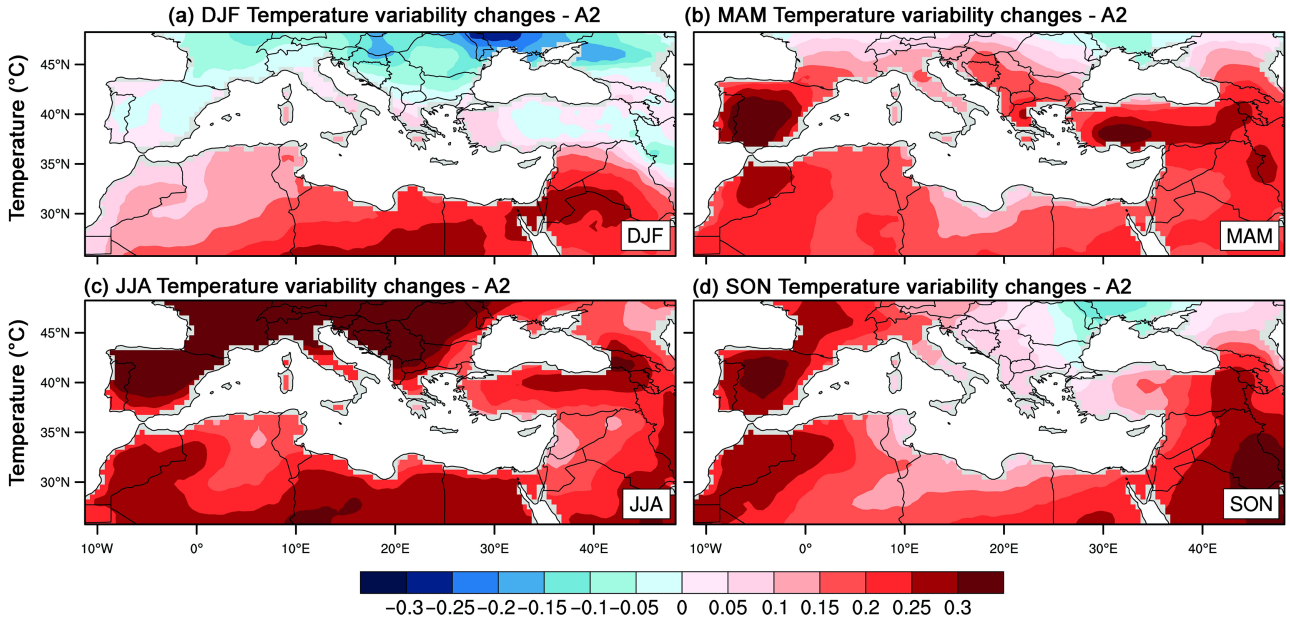

Figure 8. Ensemble average changes in inter-annual variability of surface air temperature during the future period of 2070–2100 compared to present period of 1970–2000 based on the A2 scenario for CMIP3 GCMs in (a) winter, (b) spring, (c) summer and (d) autumn.

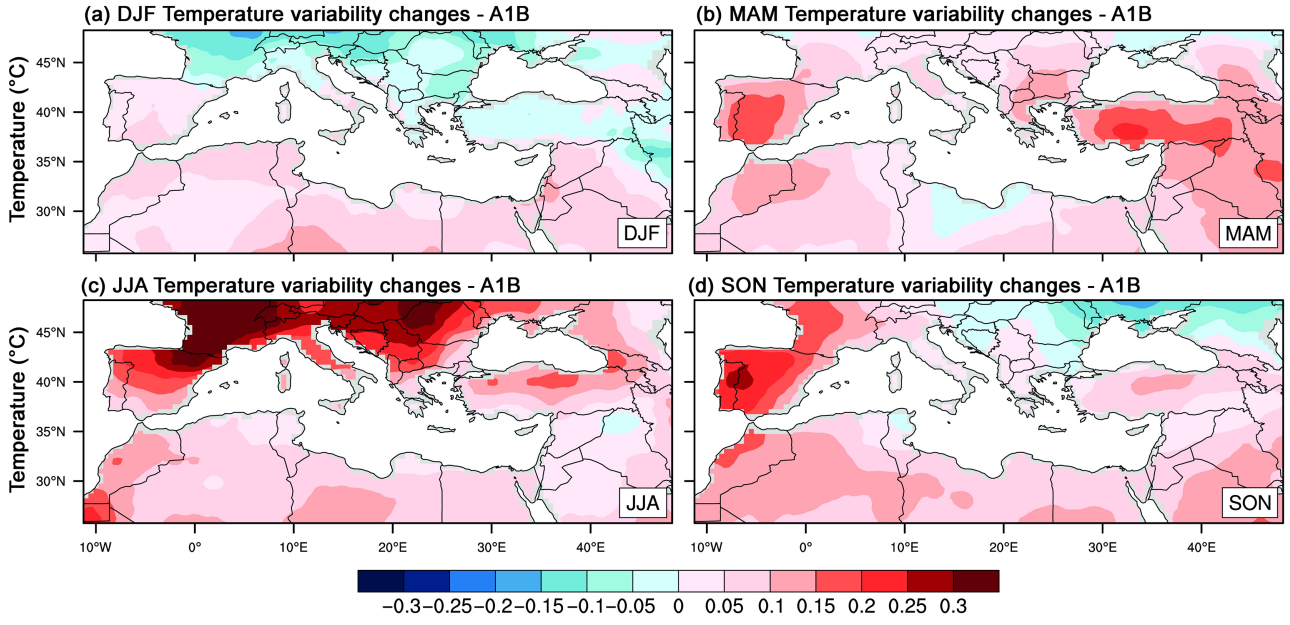

Figure 9. Ensemble average changes in inter-annual variability of surface air temperature during the future period of 2070–2100 compared to present period of 1970–2000 based on the A1B scenario for CMIP3 GCMs in (a) winter, (b) spring, (c) summer and (d) autumn.

Persistence of seasonal precipitation values is mostly statistically significant at the 0.001 level of significance except for the autumn season that is statistically significant at the 0.01 level of significance.

As for the air temperature, we see that the PDFs of reference period are symmetric and narrow (Figure 14). A2 scenario PDF has shifted the mean, wider and flattened shape of PDF compared to PDF of reference period especially in the summer season. PDF of scenario outputs for autumn and spring seasons are skewed right whereas winter season is skewed left. The shape of the distributions becomes asymmetric starting from B1 to A2 scenario output. This indicates that the occurrence and intensity of higher temperatures will increase with respect to mean temperatures. Intense weather conditions will occur more frequently in the future period with respect to the reference period. These intense weather conditions will occur especially in summer months.

The PDF of the seasonal precipitation anomalies for future and past periods are shown in Figure 15. PDFs of reference period are relatively symmetric for all seasons. There will be a decrease in precipitation mostly in the summer season according to all scenario results. Scenario PDFs become flattened and shifted slightly to the left

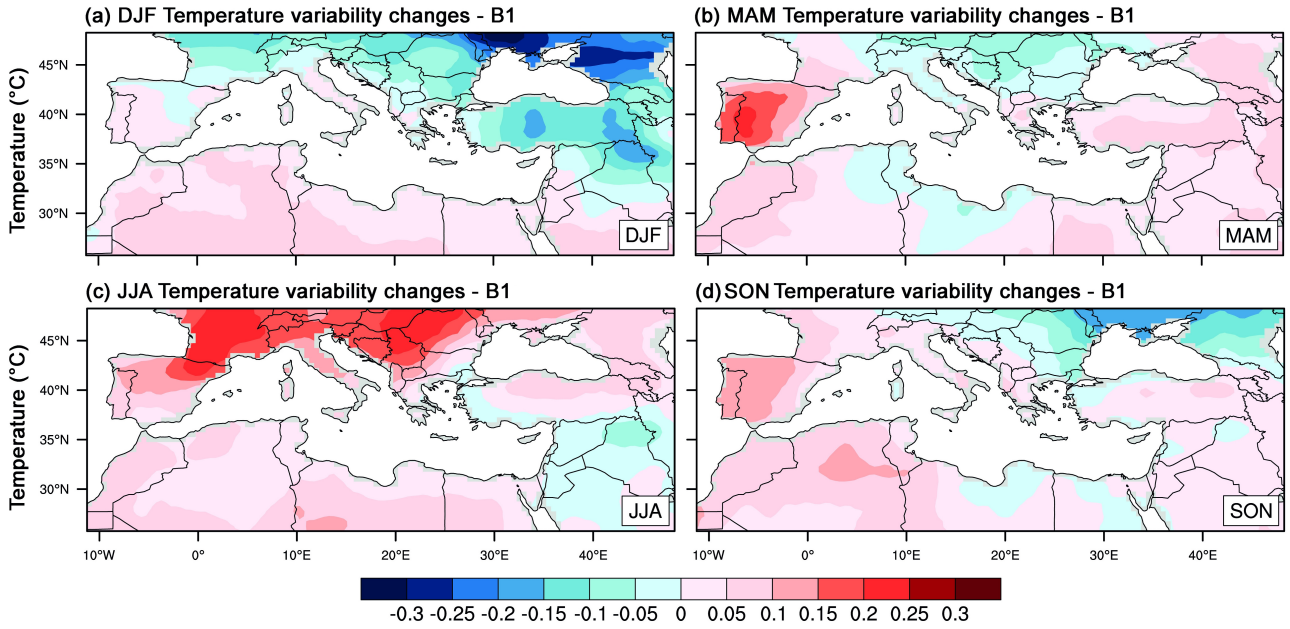

Figure 10. Ensemble average changes in inter-annual variability of surface air temperature during the future period of 2070–2100 compared to present period of 1970–2000 based on the B1 scenario for CMIP3 GCMs in (a) winter, (b) spring, (c) summer and (d) autumn.

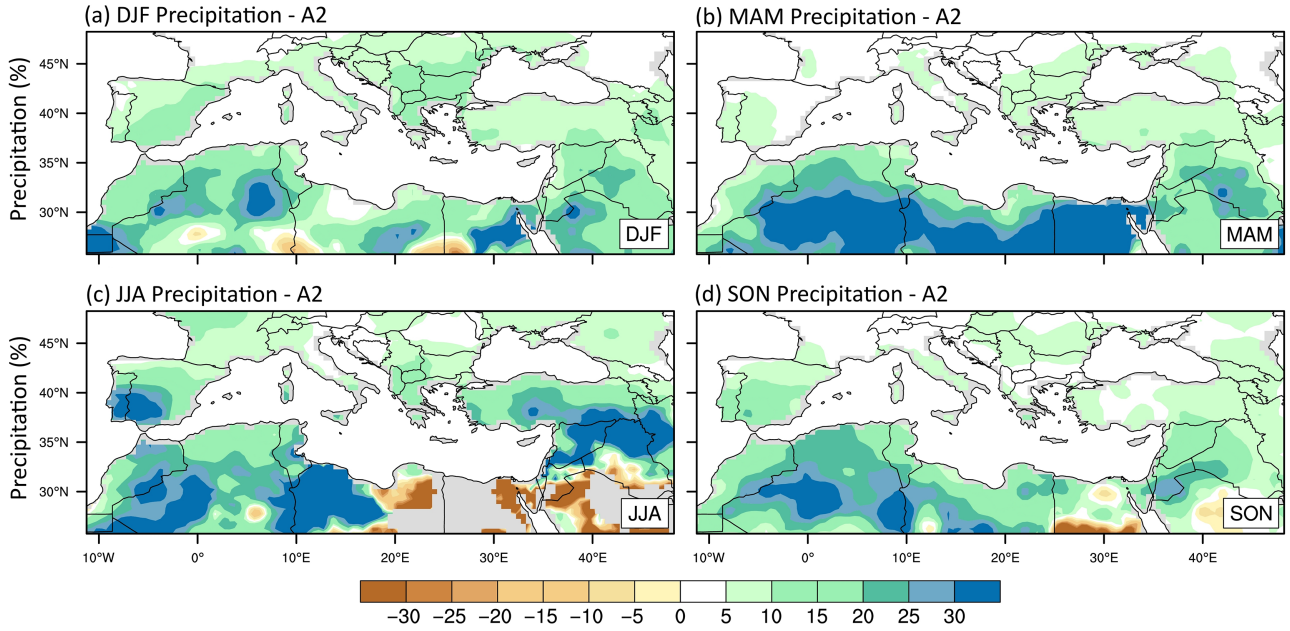

Figure 11. Ensemble average changes in inter-annual precipitation variability during the future period of 2070–2100 compared to present period of 1970–2000 based on the A2 scenario for CMIP3 GCMs in (a) winter, (b) spring, (c) summer and (d) autumn.

indicating that intense drying conditions will occur more frequently with respect to the reference period.

4. Conclusions and discussion

The present study analysed and investigated the future climate change projections of mean air temperature and precipitation climatology and variability over the Mediterranean region by using ensemble GCM outputs. A2, A1B and B1 scenario outputs of 16 global models are used to investigate climate signal for future period of 2070–2100 with respect to reference period of 1970–2000. Even though there are past studies using ensembles of many GCMs, the resolutions of the model outputs are not as fine as 50 km, which we used in this study.

We analysed ensemble average future climate change comparing to reference period. Warming trend in ensemble average model outputs for future period with respect to reference period was observed as found by previous studies (e.g. Gao and Giorgi, 2008; Giorgi and Lionello, 2008). The magnitude of future climate change signal depends on emission scenarios. Warming is maximum

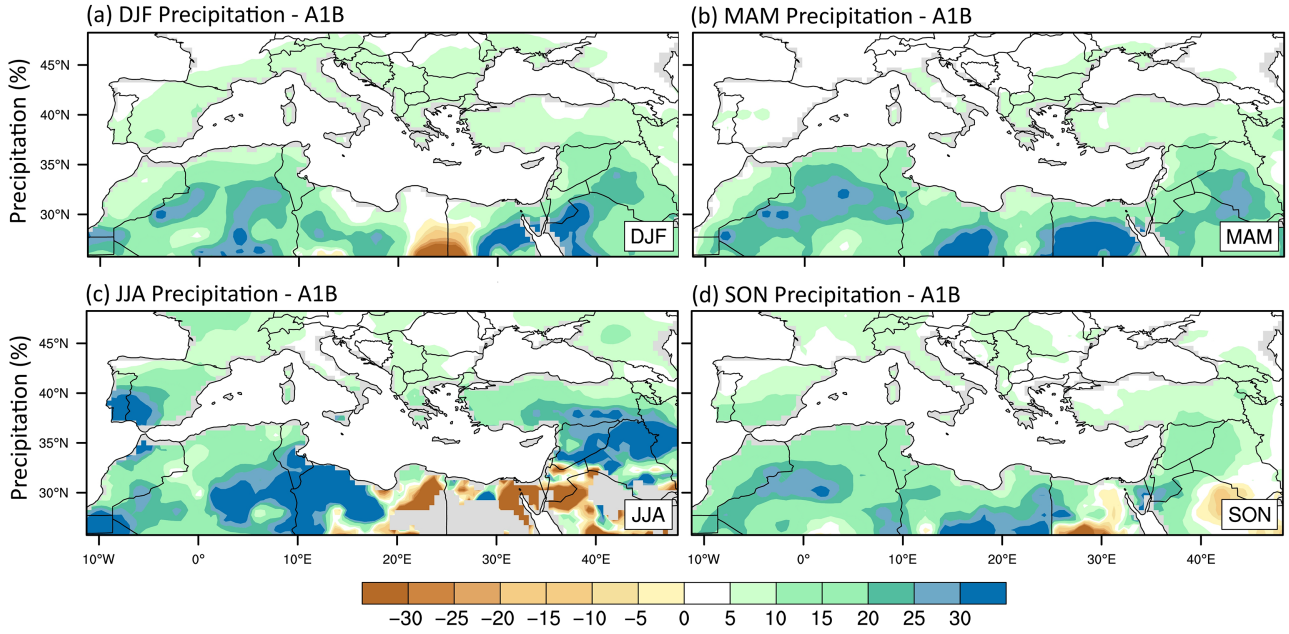

Figure 12. Ensemble average changes in inter-annual precipitation variability during the future period of 2070–2100 compared to present period of 1970–2000 based on the A1B scenario for CMIP3 GCMs in (a) winter, (b) spring, (c) summer and (d) autumn.

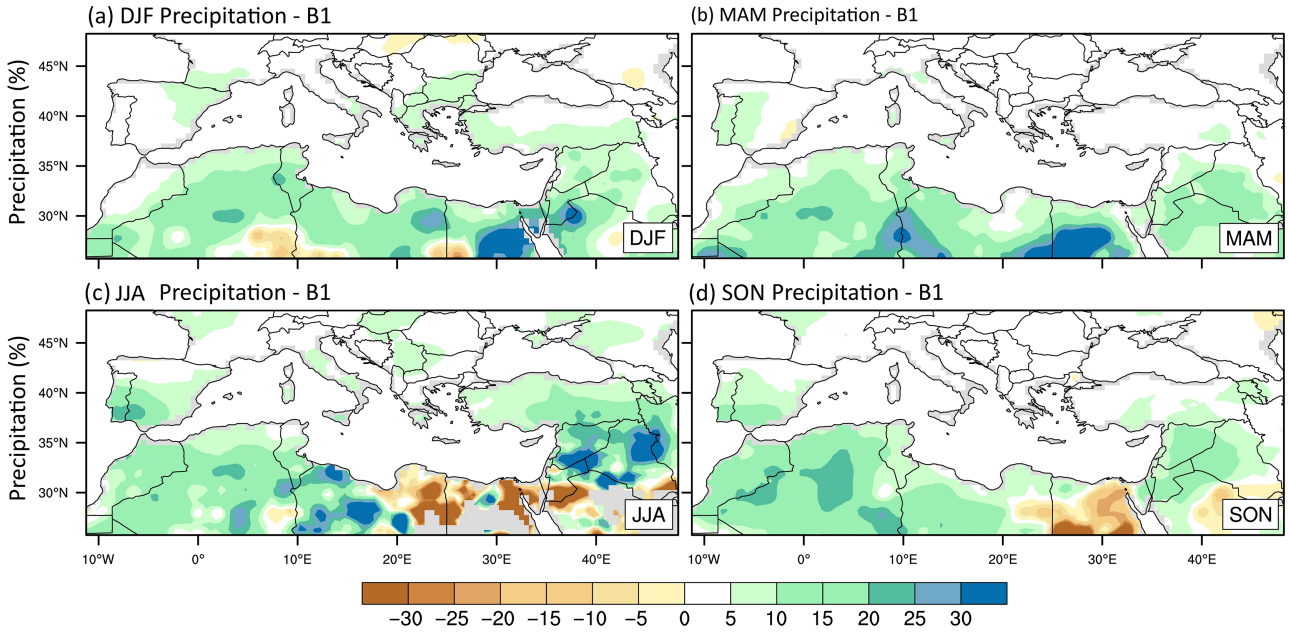

Figure 13. Ensemble average changes in inter-annual precipitation variability during the future period of 2070–2100 compared to present period of 1970–2000) based on the B1 scenario for CMIP3 GCMs in (a) winter, (b) spring, (c) summer and (d) autumn.

in summer up to 6.5 °C and minimum during the winter season.

Precipitation decreases in all seasons except increase in Switzerland during the winter season according to ensemble average of GCM outputs, as also found by other studies (e.g. Pal *et al.*, 2004; Gao *et al.*, 2006; Giorgi, 2006; Gao and Giorgi, 2008; Giorgi and Lionello, 2008; Lelieveld *et al.*, 2012). According to figure 5 of the study by Tebaldi and Arblaster, 2014', these results are also consistent with the results of CMIP5 future simulations as well. Even though CMIP3 and CMIP5 future simulations used a different set of scenarios of future greenhouse gas emission pathways, the large-scale features of the patterns obtained from CMIP3 are very similar to the ones obtained from CMIP5 experiments especially for the Mediterranean region. Decrease in precipitation amounts and marked warming were also projected in CMIP5 future simulations. Ensemble average future change signals are generally greater than the inter-model standard deviation that is agreed with previous model experiments (Jones *et al.*, 1997; Kittel *et al.*, 1998; Giorgi *et al.*, 2001). Future climate change signals can be considered as robust. For

Table 3. Results of the Levene and Student's *t*-tests for statistical significance of equality of variances and means (long-term averages) of seasonal values of air temperatures and precipitation totals for reference and A2 scenario output.

		Levene's test for equality of variances		Sudent's *t*-test for equality of means						
		F	Sig.	*t*	df	Sig. (two-tailed)	Mean difference	Std. error difference	95% confidence interval of the difference	
									Lower	Upper
MAMT	Equal variances assumed	143.72	.000	−76.73	974	.000	−3.66	.05	−3.75	−3.57
	Equal variances not assumed			−76.08	749.85	.000	−3.66	.05	−3.75	−3.57
JJAT	Equal variances assumed	331.71	.000	−91.73	974	.000	−4.79	.05	−4.89	−4.69
	Equal variances not assumed			−90.60	607.31	.000	−4.79	.05	−4.89	−4.69
SONT	Equal variances assumed	200.66	.000	−86.66	974	.000	−4.04	.05	−4.14	−3.95
	Equal variances not assumed			−85.84	714.14	.000	−4.04	.05	−4.14	−3.95
DJFT	Equal variances assumed	35.24	.000	−62.24	974	.000	−3.24	.05	−3.35	−3.14
	Equal variances not assumed			−61.96	893.18	.000	−3.24	.05	−3.35	−3.14
MAMP	Equal variances assumed	25.73	.000	15.74	974	.000	.20	.01	.17	.22
	Equal variances not assumed			15.68	914.86	.000	.20	.01	.17	.22
JJAP	Equal variances assumed	13.77	.000	23.04	974	.000	.22	.01	.21	.24
	Equal variances not assumed			22.97	920.68	.000	.22	.01	.21	.24
SONP	Equal variances assumed	15.43	.000	15.13	974	.000	.19	.012	.16	.21
	Equal variances not assumed			15.08	921.41	.000	.19	.013	.16	.21
DJFP	Equal variances assumed	26.38	.000	9.04	974	.000	.13	.014	.10	.16
	Equal variances not assumed			9.01	905.31	.000	.13	.014	.10	.16

inter-annual variability change of temperature, there will be an increase in the summer season, whereas decrease for the northern part of our domain in the winter season. Increase in precipitation variability is also observed from the model results for all seasons in the whole domain except for the south-eastern part. These results correspond to an increase in frequency of higher temperature and heavy precipitation.

Additionally, we have investigated future change of PDFs of seasonal anomalies for temperature and precipitation of the larger Mediterranean region. Seasonal anomalies for temperature and precipitation are normally distributed according to the Chi-square normality test. According to the results of normality test, except in summer for the A2 scenario output, seasonal temperature anomalies for reference and future period scenario outputs are normally distributed. In the case of precipitation anomalies, except in summer for the A1B scenario output, it is also normally distributed for reference and future periods for all scenario outputs. The values of skewness and kurtosis also indicate that seasonal temperature and precipitation anomalies are normally distributed. For temperature, the change in skewness and the shape of the distributions have indicated an increase in occurrence and intensity of higher temperatures with respect to mean temperatures. Especially in summer, it is very likely that extreme climatic conditions will be more severe in the Mediterranean Basin. The seasonal precipitation anomalies are shifted to the left indicating a decrease in mean precipitation amounts. PDFs of scenario output become flattened indicating that increased drought conditions and heavy precipitation events will very likely occur more frequently with respect to the reference period. Finally, statistical tests' results have indicated that averages and variances of temperature and precipitation will be able to change significantly in future periods with

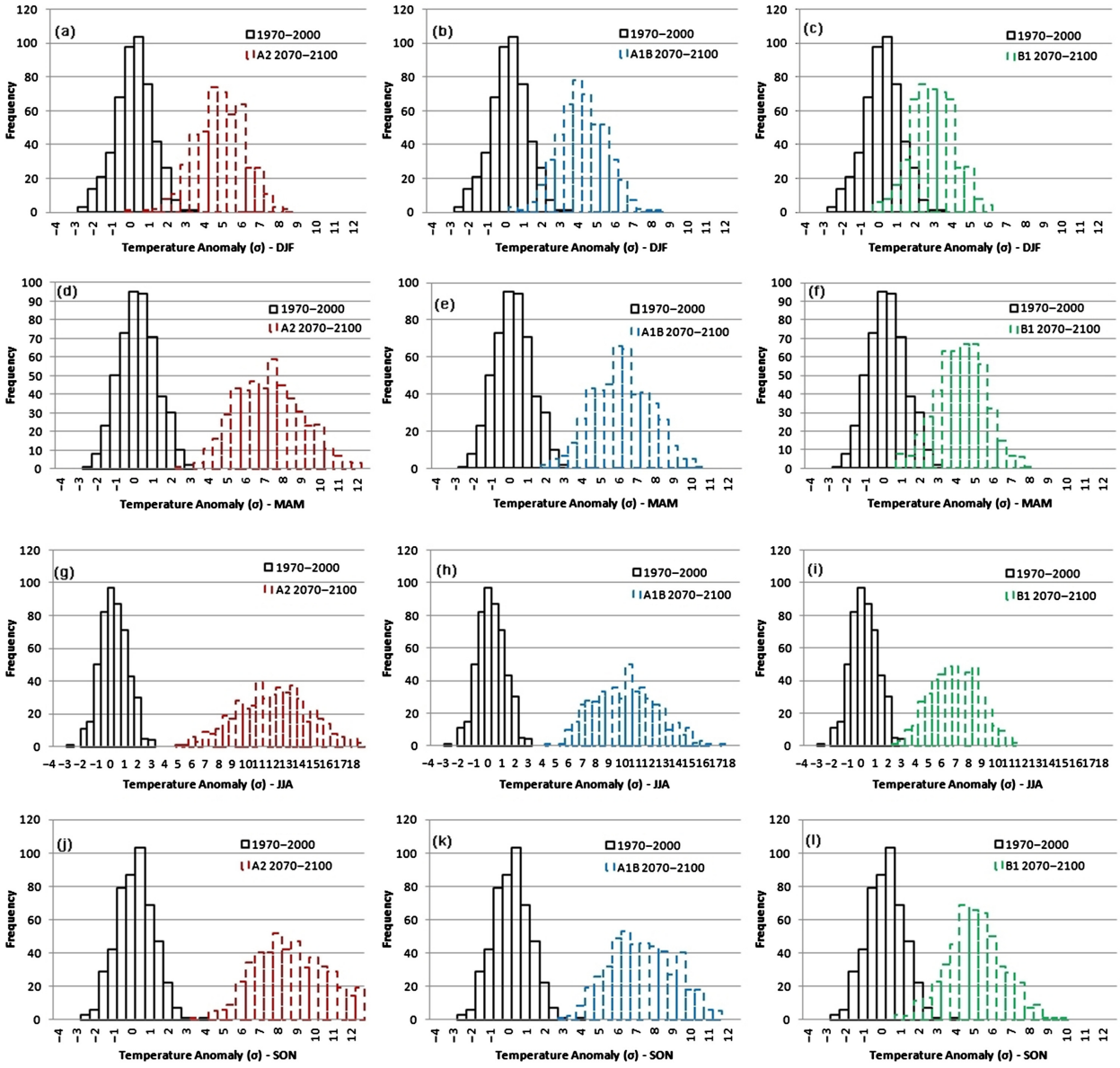

Figure 14. Statistical distribution patterns of seasonal surface air temperature anomalies in the CMIP3 GCMs for the present 1970–2000 period (simple line) and future 2070–2100 period (dashed line) based on the A2 scenario, A1B scenario and B1 scenario in winter (a, b, c), spring (d, e, f), summer (g, h, i) and autumn (j, k, l) seasons. The anomaly values are shown in σ units.

respect to the reference period. Therefore, the larger Mediterranean Basin will have warmer and dryer climate conditions in the future periods compared with the present climatology.

In this study, we verified the results of previous studies by using finer-scale GCM outputs. Findings of this study were in agreement with results obtained in past studies. However, vast majority of past studies did not include Turkey and the surrounding regions totally. Eastern Mediterranean, Turkey and Caucasian regions were also included in this work. Additionally, the change in future climatic conditions in Mediterranean region was investigated by using statistical tests. We focused on future change in seasonal climate anomalies as well.

The results shortly given above are of great importance in terms of hydrological systems, water resources, drinking water, forestry and forest fires, and soil moisture, soil organic matter content and agricultural production in the Mediterranean countries including the Northern Africa and Middle East regions and Turkey, and impacts of the global- and regional-scale observed and estimated climate changes in these regions. As a consequence of the increased meteorological droughts and associated agricultural and hydrological droughts, shortages in the water resources and losses in crop yields can also be expected. Even though the amounts of decrease in precipitation totals are somehow little, as the Mediterranean region has also mostly semi-humid, dry sub-humid and semi-arid climates with strong and long summer dryness, it will be very likely affected with a little decrease in precipitation total value. While, on the other hand, much of the desertification processes are attributed to poor land-use practices, land

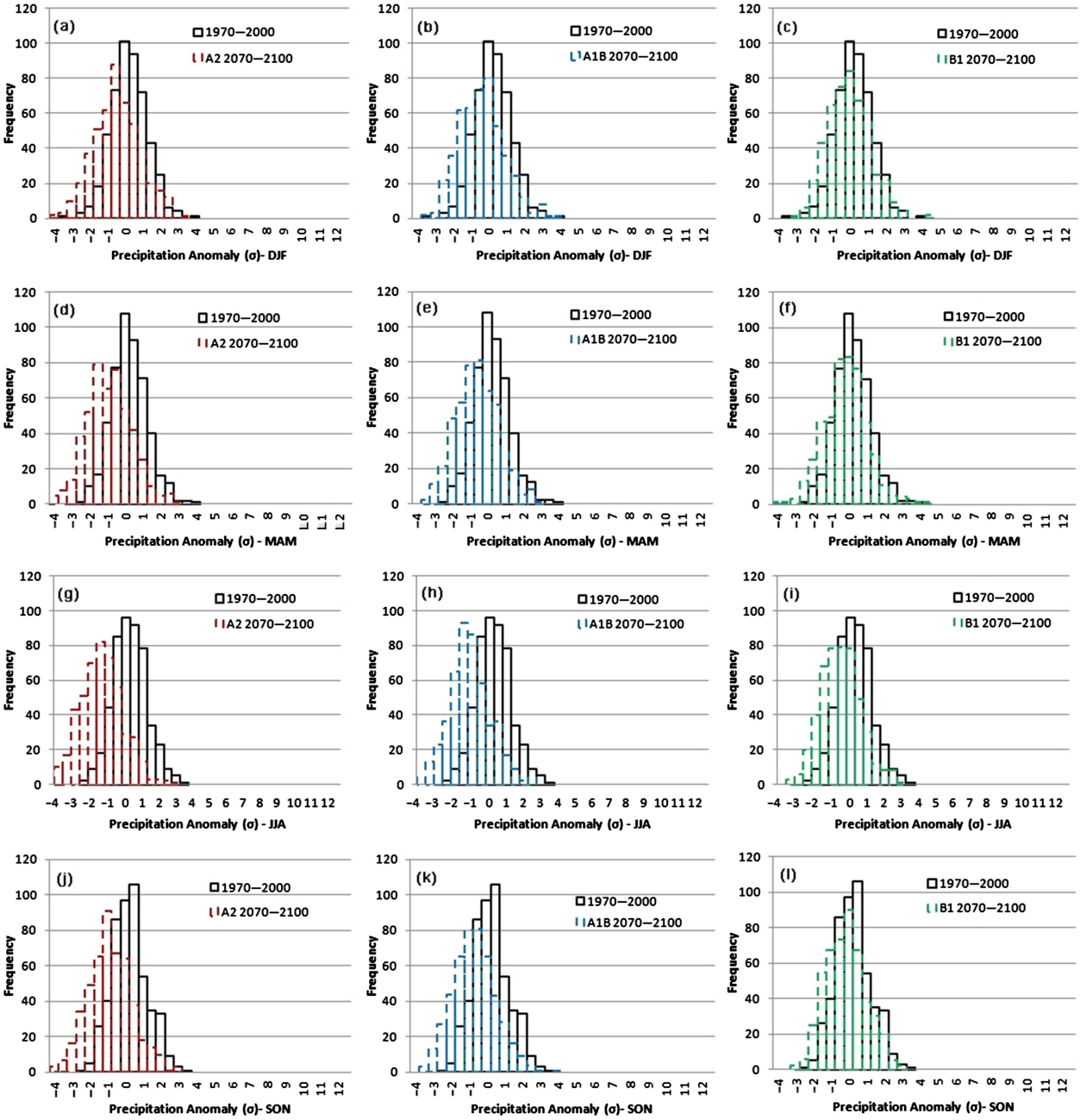

Figure 15. As in the Figure 14, but for seasonal precipitation anomalies.

degradation and climate changes particularly in arid, semi-arid and dry-subhumid regions, hotter and drier conditions will likely extend the desertification-prone areas northwards in the Mediterranean Basin to encompass areas currently not at risk. In addition, the rate of desertification would increase due to increases in erosion, salinization and forest fire hazard and reductions in soil quality. It is also likely that the first significant impacts of climate change will likely be felt in the Mediterranean hydrology and water resources systems including increased frequency of water shortages and droughts and decline in water quality.

The fifth scientific assessment report of the IPCC (Stocker *et al.*, 2013) also stated that areas with abundant atmospheric moisture availability and high present-day temperatures, such as the coastal regions of the Mediterranean Sea, are expected to experience the greatest heat stress changes. It is very likely due to the heat stress response scales with humidity, which thus will become increasingly important to heat stress at higher temperatures. The large-scale drying in the Mediterranean Basin, southwest United States, and southern Africa appear across generations of projections and climate models, and is deemed likely as global temperatures rise, and would increase the risk of severe drought events and the related disasters. Therefore, the Mediterranean Basin is a large region that is most vulnerable to climate change. The projected warming and decrease in precipitation for the domain might strongly affect the ecological and socio-economic systems of the region, which has

Table 4. Comparable representation of the descriptive statistics of minima (Min, in °C), maxima (Max in °C), long-term averages (Av in °C), standard errors of the long-term averages (SEAv in °C), standard deviations (StD in °C) and coefficients of variation (CV in %), and values of the skewness (Skew) and kurtosis (Kur) and the lag-one autocorrelation coefficients (R_L) calculated for the year-monthly overall temperature series of the MAMT, MAMA2T, MAMB1T, MAMA1BT, JJAT, JJAA2T, JJAB1T, JJAA1BT, SONT, SONA2T, SONB1T, SONA1BT, DJFT, DJFA2T, DJFB1T and DJFA1BT temperature data.[a]

Parameter	*N*	Min	Max	Av	SEAv	Skew	Kur	StD	CV	R_{L1}[b]
MAMT	496	14.094	16.729	15.409	0.023	0.094	−0.359	0.519	3.369	0.000
MAMA2T	480	16.477	21.624	19.068	0.042	0.175	−0.390	0.922	4.834	0.569***
MAMB1T	480	15.689	19.505	17.510	0.031	−0.063	−0.127	0.684	3.907	0.439***
MAMA1BT	480	16.256	20.782	18.481	0.038	0.056	−0.387	0.827	4.475	0.519***
JJAT	496	23.963	26.368	25.217	0.018	0.115	−0.215	0.407	1.615	0.201***
JJAA2T	480	27.192	32.902	30.006	0.050	−0.012	−0.407	1.087	3.621	0.805***
JJAB1T	480	26.131	29.897	27.961	0.033	0.041	−0.519	0.728	2.605	0.714***
JJAA1BT	480	26.977	32.139	29.287	0.043	0.212	−0.476	0.949	3.240	0.789***
SONT	496	15.660	18.802	17.084	0.021	−0.064	0.015	0.477	2.792	0.200***
SONA2T	480	18.703	23.498	21.128	0.042	0.158	−0.539	0.919	4.351	0.698***
SONB1T	480	17.465	21.662	19.395	0.033	0.094	0.021	0.721	3.719	0.603***
SONA1BT	480	18.282	22.543	20.486	0.038	0.121	−0.634	0.836	4.079	0.671***
DJFT	496	4.839	8.974	6.856	0.031	−0.175	0.092	0.697	10.173	0.190***
DJFA2T	480	6.793	12.606	10.100	0.042	−0.163	0.020	0.919	9.100	0.427***
DJFB1T	480	6.606	11.023	8.778	0.037	−0.036	−0.150	0.816	9.293	0.365***
DJFA1BT	480	6.992	12.439	9.651	0.041	0.035	−0.070	0.897	9.294	0.387***

[a]MAMT, spring temperature for reference period; MAMA2T, spring temperature for future period of 2070–2100 based on A2 scenario; MAMB1T, spring temperature for future period of 2070–2100 based on B1 scenario; MAMA1BT, spring temperature for future period of 2070–2100 based on A1B scenario, summer, autumn and winter, respectively (JJAT, JJAA2T, JJAB1T, JJAA1BT, SONT, SONA2T, SONB1T, SONA1BT, DJFT, DJFA2T, DJFB1T and DJFA1BT).

[b]Statistical significance of R_L was controlled by using the Box-Ljung test statistic based on the approximation of the asymptotic Chi-square distribution.

Statistically significant at the *0.05, **0.01 and ***0.001 levels of significance.

Table 5. Comparable representation of the descriptive statistics of minima (Min, in mm day^{-1}), maxima (Max in mm day^{-1}), long-term averages (Av in mm day^{-1}), standard errors of the long-term averages (SEAv in mm day^{-1}), standard deviations (StD in mm day^{-1}) and coefficients of variation (CV in %), and values of the skewness (Skew) and kurtosis (Kur) and the lag-one autocorrelation coefficients (R_L) calculated for the year-monthly overall temperature series of the MAMP, MAMA2P, MAMB1P, MAMA1BP, JJAP, JJAA2P, JJAB1P, JJAA1BP, SONP, SONA2P, SONB1P, SONA1BP, DJFP, DJFA2P, DJFB1P and DJFA1BP precipitation data.[a]

Parameter	*N*	Min	Max	Av	SEAv	Skew	Kur	StD	CV	R_{L1}[b]
MAMP	496	0.820	1.950	1.306	0.008	0.306	0.458	0.175	13.366	0.000
MAMA2P	480	0.460	1.760	1.107	0.010	0.200	0.059	0.219	19.770	0.208***
MAMB1P	480	0.580	2.030	1.238	0.010	0.246	0.685	0.211	17.013	0.152***
MAMA1BP	480	0.610	1.760	1.161	0.010	0.242	−0.037	0.210	18.084	0.134***
JJAP	496	0.470	1.280	0.843	0.006	0.185	0.020	0.136	16.068	0.027**
JJAA2P	480	0.180	1.240	0.619	0.008	0.291	0.330	0.167	27.047	0.461***
JJAB1P	480	0.330	1.180	0.734	0.007	0.265	0.101	0.154	20.955	0.185***
JJAA1BP	480	0.260	1.140	0.658	0.007	0.320	0.064	0.162	24.573	0.378***
SONP	496	0.820	1.840	1.260	0.008	0.218	−0.079	0.173	13.740	0.026**
SONA2P	480	0.410	1.740	1.072	0.010	0.179	0.219	0.214	19.915	0.096**
SONB1P	480	0.670	1.710	1.186	0.009	0.132	−0.377	0.193	16.257	0.065**
SONA1BP	480	0.600	1.880	1.102	0.010	0.306	0.174	0.209	18.937	0.023**
DJFP	496	0.830	2.210	1.514	0.009	0.070	0.332	0.192	12.652	0.057**
DJFA2P	480	0.650	2.150	1.386	0.011	0.132	−0.095	0.246	17.711	0.153***
DJFB1P	480	0.940	2.340	1.459	0.010	0.383	0.362	0.223	15.260	0.114***
DJFA1BP	480	0.750	2.260	1.397	0.011	0.403	0.249	0.242	17.297	0.246***

[a]MAMT, spring temperature for reference period; MAMA2T, spring temperature for future period of 2070–2100 based on A2 scenario; MAMB1T, spring temperature for future period of 2070–2100 based on B1 scenario; MAMA1BT, spring temperature for future period of 2070–2100 based on A1B scenario, summer, autumn and winter, respectively (JJAT, JJAA2T, JJAB1T, JJAA1BT, SONT, SONA2T, SONB1T, SONA1BT, DJFT, DJFA2T, DJFB1T and DJFA1BT).

[b]Statistical significance of R_L was controlled by using the Box-Ljung test statistic based on the approximation of the asymptotic Chi-square distribution.

Statistically significant at the *0.05, **0.01 and ***0.001 levels of significance.

already been characterized mostly with a semi-arid and dry-sub-humid or semi-humid environment.

Acknowledgements

This work has been supported by Bogazici University BAP under project number 7362. One of the authors (MLK) was partly supported by Mercator-IPC Fellowship Program.

References

Adam JC, Lettenmaier DP. 2003. Adjustment of global gridded precipitation for systematic bias. *J. Geophys. Res.* **108**: 4257–4270.

Alpert P, Krichak SO, Shafir H, Haim D, Osetinsky I. 2008. Climatic trends to extremes employing regional modeling and statistical interpretation over the E. Mediterranean. *Glob. Planet. Change* **63**: 163–170.

Barnett TP, Pierce DW, Hidalgo HG, Bonfils C, Santer BD, Das T, Bala G, Wood AW, Nozawa T, Mirin AA, Cayan DR, Dettinger MD. 2008. Human-induced changes in the hydrology of the western United States. *Science* **319**(5866): 1080–1083.

Beniston M, Stephenson DB, Christensen OB, Ferro CAT, Frei C, Goyette S, Halsnaes K, Holt T, Jylha K, Koffi B, Palutikof J, Scholl R, Semmler T, Woth K. 2007. Future extreme events in European climate: an exploration of regional climate model projections. *Clim. Change* **81**: 71–95.

Buffoni L, Maugeri M, Nanni T. 1999. Precipitation in Italy 1833 to 1996. *Theor. Appl. Climatol.* **63**: 33–40.

Buffoni L, Maugeri M, Nanni T. 2000. Variation of temperature and precipitation in Italy from 1866 to 1995. *Theor. Appl. Climatol.* **65**: 165–174.

Christensen JH, Christensen OB. 2003. Climate modeling: severe summertime flooding in Europe. *Nature* **421**: 805–806.

Coppola E, Giorgi F. 2010. An assessment of temperature and precipitation change projections over Italy from recent global and regional climate model simulations. *Int. J. Climatol.* **30**: 11–32.

Deque M, Marquet P, Jones RG. 1998. Simulation of climate change over Europe using a global variable resolution general circulation model. *Clim. Dyn.* **14**: 173–189.

Deque M, Jones RG, Wild M, Giorgi F, Christensen H, Hassell DC, Vidale PL, Rockel B, Jacob D, Kjellstrom E, de Castro M, Kucharski F, van den Hurk B. 2005. Global high resolution vs. regional climate model climate change scenarios over Europe: quantifying confidence level from PRUDENCE results. *Clim. Dyn.* **25**: 653–670.

Esteban-Parra MJ, Rodrigo FS, Castro-Diez Y. 1998. Spatial and temporal patterns of precipitation in Spain for the period 1880–1992. *Int. J. Climatol.* **14**: 1557–1574.

Gao X, Giorgi F. 2008. Increased aridity in the Mediterranean region under greenhouse gas forcing estimated from high resolution regional climate projections. *Glob. Planet. Chang.* **62**: 195–209.

Gao X, Pal JS, Giorgi F. 2006. Projected changes in mean and extreme precipitation over the Mediterranean region from high resolution double nested RCM simulations. *Geophys. Res. Lett.* **33**: L03706.

Giorgi F. 2002. Variability and trends of sub-continental scale surface climate in the twentieth century, part I: observations. *Clim. Dyn.* **18**: 675–691.

Giorgi F. 2006. Climate change hot-spots. *Geophys. Res. Lett.* **33**: L08707, doi: 10.1029/2006GL025734.

Giorgi F, Bi X. 2005a. Regional changes in surface climate interannual variability for the 21st century from ensembles of global model simulations. *Geophys. Res. Lett.* **32**: L13701.

Giorgi F, Bi X. 2005b. Updated regional precipitation and temperature changes for the 21st century from ensembles of recent AOGCM simulations. *Geophys. Res. Lett.* **32**: L21715.

Giorgi F, Francisco R. 2000. Evaluating uncertainties in the prediction of regional climate change. *Geophys. Res. Lett.* **27**: 1295–1298.

Giorgi F, Lionello P. 2008. Climate change projections for the mediterranean region. *Glob. Planet. Chang.* **63**: 90–104.

Giorgi F, Marinucci MR, Visconti G. 1992. A $2XCO_2$ climate change scenario over Europe generated using a limited area model nested in a general circulation model, II: climate change scenario. *J. Geophys. Res.* **97**: 10011–10028.

Giorgi F, Hurrell JW, Marinucci MR, Beniston M. 1997. Elevation signal in surface climate change: a model study. *J. Clim.* **10**: 288–296.

Giorgi F, Whetton PH, Jones RG, Christensen JH, Mearns LO, Hewitson B, von Storch H, Francisco R, Jack C. 2001. Emerging patterns of simulated regional climatic changes for the 21st century due to anthropogenic forcings. *Geophys. Res. Lett.* **28**: 3317–3320.

Giorgi F, Bi X, Pal JS. 2004. Mean, interannual variability and trends in a regional climate change experiment over Europe, part II: future climate scenarios (2071–2100). *Clim. Dyn.* **23**: 839–858.

Gonzalez-Rouco JF, Heyen H, Zorita E, Valero F. 2000. Agreement between observed rainfall trends and climate change simulations in Southern Europe. *J. Clim.* **13**: 3057–3065.

Gonzalez-Rouco JF, Jimenez JL, Quesada V, Valero F. 2001. Quality control and homogenization of monthly precipitation data in the southwest of Europe. *J. Clim.* **14**: 964–978.

Hayhoe K, Wake C, Anderson B, Liang X-Z, Maurer E, Zhu J, Bradbury J, DeGaetano A, Stoner A, Wuebbles D. 2007. Regional climate change projections for the Northeast USA. *Mitig. Adapt. Strateg. Glob. Chang.* **13**: 425–436. 10.1007/s11027-007-9133-2.

Houghton JTY, Ding Y, Griggs DJ, Noguer M, van der Linden PJ, Dai X, Maskell K, Johnson CA (eds). 2001. *Climate Change 2001: The Scientific Basis. Contribution of Working Group I to the Third Assessment Report of the Intergovernmental Panel on Climate Change*. Cambridge University Press: Cambridge, UK and New York, NY, 881 pp.

Hurrell JW, Kushnir Y, Ottersen G, Visbeck M. 2003. An overview of the North Atlantic Oscillation. *Geophys. Monogr. Ser.* **134**: 1–35.

Jones RG, Murphy JM, Noguer M, Keen AB. 1997. Simulation of climate change over Europe using a nested regional climate model, II: comparison of driving and regional model responses to a doubling of carbon dioxide. *Q. J. R. Meteorol. Soc.* **123**: 265–292.

Kidson JW, Thompson CS. 1998. A comparison of statistical and model-based downscaling techniques for estimating local climate variations. *J. Clim.* **11**: 735–753.

Kittel TGF, Giorgi F, Meehl GA. 1998. Intercomparison of regional biases and doubled CO2 sensitivities of coupled atmosphere–ocean general circulation model experiments. *Clim. Dyn.* **14**: 1–15.

Kjellstrom E. 2004. Recent and future signatures of climate change in Europe. *Ambio* **33**: 193–198.

Kjellstrom E, Barring L, Jacob D, Jones R, Lenderink G, Schär C. 2007. Modeling daily temperature extremes: recent climate and future changes over Europe. *Clim. Change* **81**: 249–265.

Kripalani RH, Oh JH, Kulkarni A, Sabade SS, Chaudhari HS. 2007. South Asian summer monsoon precipitation variability: coupled climate model simulations and projections under IPCC AR4. *Theor. Appl. Climatol.* **90**: 133–159.

Kutiel H, Türkeş M. 2005. New evidence for the role of the North Sea–Caspian Pattern on the temperature and precipitation regimes in continental central Turkey. *Geogr. Ann. Ser. A Phys. Geogr.* **87**: 501–513.

Kutiel H, Maheras P, Türkeş M, Paz S. 2002. North Sea–Caspian Pattern (NCP) – an upper level atmospheric teleconnection affecting the eastern Mediterranean – implications on the regional climate. *Theor. Appl. Climatol.* **72**: 173–192.

Lelieveld J, Hadjinicolaou P, Kostopoulou E, Chenoweth J, Giannakopoulos C, Hannides C, Lange MA, El Maayar M, Tanarthe M, Tyrlis E, Xoplaki E. 2012. Climate change and impacts in the eastern Mediterranean and the Middle East. *Clim. Change* **114**: 667–687.

Machenhauer B, Windelband M, Botzet M, Christensen JH, Deque M, Jones RG, Ruti PM, Visconti G. 1998. Validation and analysis of regional present-day climate and climate change simulations over Europe. Report, No. 275, Max Planck Institute for Meteorology, Hamburg, Germany.

Maurer EP, Duffy PB. 2005. Uncertainty in projections of streamflow changes due to climate change in California. *Geophys. Res. Lett.* **32**: L03704, doi: 10.1029/2004GL021462.

Maurer EP, Hidalgo HG. 2007. Utility of daily vs. monthly large-scale climate data: an intercomparison of two statistical downscaling methods. *Hydrol. Earth Syst. Sci.* **12**: 551–563.

Maurer EP, Adam JC, Wood AW. 2009. Climate model based consensus on the hydrologic impacts of climate change to the Rio Lempa basin of Central America. *Hydrol. Earth Syst. Sci.* **13**: 183–194.

Meehl GA, Covey C, Delworth T, Latif M, Mcavaney B, Mitchell JFB, Stouffer RJ, Taylor KE. 2007. The WCRP CMIP3 multi-model dataset: a new era in climate change research. *Bull. Am. Meteorol. Soc.* **88**: 1383–1394.

Murphy J. 1999. An evaluation of statistical and dynamical techniques for downscaling local climate. *J. Clim.* **12**: 2256–2284.

Nakicenovic N, Swart R (eds). 2000. *Special Report on Emissions Scenarios (SRES) – A Special Report of Working Group III of the Intergovernmental Panel on Climate Change*. Cambridge University Press: Cambridge, UK and New York, NY, 570 pp.

Ozturk T, Altınsoy H, Türkeş M, Kurnaz ML. 2012. Simulation of temperature and precipitation climatology for central Asia CORDEX domain by using RegCM 4.0. *Clim. Res.* **52**: 63–76.

Ozturk T, Türkeş M, Kurnaz ML. 2013. Projected changes in air temperature and precipitation climatology in Turkey by using RegCM 4.3. In *Proceedings of European Geosciences Union General Assembly 2013*, Vienna, Austria, 7–12 April.

Pal JS, Giorgi F, Bi X. 2004. Consistency of recent summer European precipitation trends an extremes with future regional climate projections. *Geophys. Res. Lett.* **31**: L13202.

Panofsky HA, Brier GW. 1968. *Some Applications of Statistics to Meteorology*. The Pennsylvania State University: University Park, PA, 224 pp.

Raisanen J, Rummukainen M, Ullerstig A, Bringfelt B, Hansson U, Willén U. 1999. The first Rossby Centre regional climate scenario – dynamical downscaling of CO_2-induced climate change in the HadCM2 GCM. SHMI Reports Meteorology and Climatology No. 85, Swedish Meteorological and Hydrological Institute, Norrkoping, Sweden, 56 pp.

Raisanen J, Hansson U, Ullerstig A, Doscher R, Graham LP, Jones C, Meier HEM, Samuelsson P, Willen U. 2004. European climate in the late twenty-first century: regional simulations with two driving global models and two forcing scenarios. *Clim. Dyn.* **22**: 13–31.

Rotach MW, Marinucci MR, Wild M, Tschuck P, Ohmura A, Beniston M. 1997. Nested regional simulation of climate change over the Alps for the scenario of doubled greenhouse gas forcing. *Theor. Appl. Climatol.* **57**: 209–227.

Schar C, Vidale PL, Luthi D, Frei C, Haberli C, Liniger MA, Appenzeller C. 2004. The role of increasing temperature variability in European summer heatwaves. *Nature* **427**: 332–336.

Semmler T, Jacob D. 2004. Modeling extreme precipitation events – a climate change simulation for Europe. *Glob. Planet. Chang.* **44**: 119–127.

Sharma D, Das Gupta A, Babel MS. 2007. Spatial disaggregation of bias-corrected GCM precipitation for improved hydrologic simulation: Ping river basin, Thailand. *Hydrol. Earth Syst. Sci.* **11**(4): 1373–1390.

Sheffield J, Wood EF. 2008. Projected changes in drought occurrence under future global warming from multi-model, multi-scenario, IPCC AR4 simulations. *Clim. Dyn.* **31**: 79–105.

Solomon S, Qin D, Manning M, Chen Z, Marquis M, Averyt KB, Tignor M, Miller HL (eds). 2007. *Climate Change 2007: The Physical Science Basis. Contribution of Working Group I to the Fourth Assessment Report of the Intergovernmental Panel on Climate Change*. Cambridge University Press: Cambridge, UK and New York, NY, 996 pp.

Stocker TF, Qin D, Plattner G-K, Tignor M, Allen SK, Boschung J, Nauels A, Xia Y, Bex V, Midgley PM (eds). 2013. *Climate Change 2013: The Physical Science Basis. Summary for Policymakers. Contribution of Working Group I to the Fifth Assessment Report of the Intergovernmental Panel on Climate Change*. Cambridge University Press: Cambridge, UK and New York, NY, 27 pp.

Tabor K, Williams JW. 2010. Globally downscaled climate projections for assessing the conservation impacts of climate change. *Ecol. Appl.* **20**: 554–565.

Tatlı H, Türkeş M. 2008. Drought events of 2006/2007 in Turkey and determination of its association with large-scale atmospheric variables by logistic regression. In *Proceedings of 4th Atmospheric Science Symposium*. İstanbul Technical University: İstanbul, Turkey, 516–527 (in Turkish with an English abstract).

Tatlı H, Türkeş M. 2011a. Examinaton of the dry and wet conditions in Turkey via model output statistics (MOS). In *Proceedings of 5th Atmospheric Science Symposium*. İstanbul Technical University: İstanbul, Turkey, 219–229 (in Turkish with an English abstract).

Tatlı H, Türkeş M. 2011b. Empirical orthogonal function analysis of the Palmer drought indices. *Agric. For. Meteorol.* **151**(7): 981–991.

Tebaldi C, Arblaster JM. 2014. Pattern-scaling: its strengths and limitations, and an update on the latest model simulations. *Clim. Change* **122**: 459–471, doi: 10.1007/s10584-013-1032-9.

Tomozeiu R, Lazzeri M, Cacciamani C. 1995. Precipitation fluctuations during the winter season from 1960 to 1995 over Emilia-Romagna, Italy. *Theor. Appl. Climatol.* **72**: 221–229.

Trigo R, Xoplaki E, Zorita E, Luterbacher J, Krichak S, Alpert P, Jacobeit J, Saenz J, Fernandez J, Gonzalez-Rouco F, Garcia-Herrera R, Rodo X, Brunetti M, Nanni T, Maugeri M, Türkeş M, Gimeno L, Ribera P, Brunet M, Trigo I, Crepon M, Mariotti A. 2006. Relations between variability in the Mediterranean region and mid-latitude variability. In *Mediterranean Climate Variability: Developments in Earth & Environmental Sciences 4*, Lionello P, Malanotte-Rizzoli P, Boscolo R (eds). Elsevier: Amsterdam, 179–226.

Türkeş M. 1998. Influence of geopotential heights, cyclone frequency and southern oscillation on rainfall variations in Turkey. *Int. J. Climatol.* **18**: 649–680.

Türkeş M. 1999. Vulnerability of Turkey to desertification with respect to precipitation and aridity conditions. *Turk. J. Eng. Environ. Sci.* **23**: 363–380.

Türkeş M. 2010. *Climatology and Meteorology*. Kriter Publisher: Istanbul, Turkey, 650 pp (in Turkish).

Türkeş M, Erlat E. 2003. Precipitation changes and variability in Turkey linked to the North Atlantic Oscillation during the period 1930–2000. *Int. J. Climatol.* **23**: 1771–1796.

Türkeş M, Erlat E. 2005. Climatological responses of winter precipitation in Turkey to variability of the North Atlantic Oscillation during the period 1930–2001. *Theor. Appl. Climatol.* **81**: 45–69.

Türkeş M, Erlat E. 2006. Influences of the North Atlantic Oscillation on precipitation variability and changes in Turkey. *Nuovo Cimento C* **29**: 117–135.

Türkeş M, Erlat E. 2008. Influence of the Arctic Oscillation on variability of winter mean temperatures in Turkey. *Theor. Appl. Climatol.* **92**: 75–85.

Türkeş M, Erlat E. 2009. Winter mean temperature variability in Turkey associated with the North Atlantic Oscillation. *Meteorog. Atmos. Phys.* **105**: 211–225.

Türkeş M, Tatlı H. 2009. Use of the standardized precipitation index (SPI) and modified SPI for shaping the drought probabilities over Turkey. *Int. J. Climatol.* **29**: 2270–2282.

Türkeş M, Tatlı H. 2011. Use of the spectral clustering to determine coherent precipitation regions in Turkey for the period 1929–2007. *Int. J. Climatol.* **31**: 2055–2067.

Türkeş M, Koç T, Sarış F. 2009. Spatiotemporal variability of precipitation total series over Turkey. *Int. J. Climatol.* **29**: 1056–1074.

Van Rheenan NT, Wood AW, Palmer RN, Lettenmaier DP. 2004. Potential implications of PCM climate change scenarios for Sacramento–San Joaquin River basin hydrology and water resources. *Clim. Change* **62**: 257–281.

Vidal JP, Wade SD. 2008. A framework for developing high-resolution multi-model climate projections: 21st century scenarios for the UK. *Int. J. Climatol.* **28**: 843–858, doi: 10.1002/joc.1593.

Wilby RL, Hay LE, Gutowski WJ Jr, Arritt RW, Takle ES, Pan Z, Leavesley GH, Clark MP. 2000. Hydrological responses to dynamically and statistically downscaled climate model output. *Geophys. Res. Lett.* **27**: 1199–1202.

Wood AW, Maurer EP, Kumar A, Lettenmaier DP. 2002. Longrange experimental hydrologic forecasting for the eastern U.S. *J. Geophys. Res.* **107**(D20): 4429–4443, doi:10.1029/2001JD000659.

Wood AW, Leung LR, Sridhar V, Lettenmaier DP. 2004. Hydrologic implications of dynamical and statistical approaches to downscaling climate model outputs. *Clim. Change* **62**: 189–216.

Xoplaki E, Luterbacher J, Burkard R, Patrikas I, Maheras P. 2000. Connection between the large-scale 500 hPa geopotential height fields and precipitation over Greece during wintertime. *Clim. Res.* **14**: 129–146.

